

Section 8

Development of and advances in ocean, sea-ice,
and wave modelling and data assimilation.

Ocean Data Impacts in the Real Time Ocean Forecast System: RTOFS-v2

James Cummings¹, Zulema Garraffo¹, Dan Iredell¹, Shastri Paturi¹, Yan Hao¹, Todd Spindler¹, Bhavani Alasubramanian¹, and Avichal Mehra²
¹IMSG at NOAA/NWS/NCEP/EMC, ²NOAA/NWS/NCEP/EMC Jim.Cummings@noaa.gov

Introduction

It is likely that not all observations assimilated have equal value in reducing ocean model forecast error. Estimation of which observations are best and the determination of locations where forecast errors are sensitive to the initial conditions are essential for improving the data assimilation system itself and for the design and implementation of future observing systems. This paper describes application of the adjoint-based procedure to estimation of the impact of observations assimilated on reducing ocean model forecast error in the Real-Time Ocean Forecast System (RTOFS-v2). The technique computes the variation in forecast error due to the assimilated data. Observation impacts are estimated simultaneously for the complete set of observations assimilated. The method is computationally inexpensive and can be used for routine observation monitoring. This aspect of the adjoint technique is advantageous since ocean observing and assimilation/forecast systems are in continuous evolution requiring an efficient procedure that allows the impact of observations to be regularly assessed. Data impacts can be partitioned for any subset of the data assimilated: instrument type, observed variable, geographic region, or vertical level, with traceability to individual platforms based on station identifying call signs. The results shown here illustrate some of the types of diagnostics that can be routinely obtained with the adjoint method in an operational context.

RTOFS-v2

The ocean forecast component of RTOFS-v2 is the Hybrid Coordinate Ocean Model (HyCOM), which is configured on a global tri-polar grid with horizontal equatorial resolution of .08° or ~1/12° (~7 km mid latitude). This configuration makes HyCOM eddy resolving. Eddy resolving is important for ocean model dynamical interpolation skill in data assimilation. HyCOM is configured with 41 hybrid vertical coordinate surfaces. The data assimilation component of RTOFS-v2 consists of a three-dimensional variational (3DVAR) analysis. The analysis variables are temperature, salinity, geopotential, and u, v vector velocity components. All variables are analyzed simultaneously in a multivariate procedure that permits adjustments to the mass fields to be correlated with adjustments to the flow fields. The 3DVAR observation vector contains all of the synoptic temperature, salinity and velocity observations received at the center within the 24-hour update cycle interval. The analysis makes full use of all sources of the operational ocean observations. RTOFS-v2 routinely assimilates about 2 million observations per day onto the global HyCOM grid, which contains more than 520 million grid points.

Adjoint Procedure

Adjoint-based observation sensitivity provides a feasible all at once approach to estimating observation impact. Observation impact depends on the forecast error metric, the innovations (model-data differences at the update cycle interval), and the number of observations. Since forecast errors grow and decay at different rates throughout the model domain, a large model-data difference does not necessarily lead to a large data impact. Observations can make small changes to the initial conditions and still have a large data impact if the location of the observation is in a dynamically sensitive region. Here, the forecast error metric is defined as the difference between forecasts of 48 and 72 hours valid at the same time. Forecast errors result from inaccuracies in the initial conditions, the atmospheric forcing, and the non-linear forecast model. However, differences between forecast errors from forecasts of different lengths verifying at the same time are solely due to the assimilation of observations, which makes it an appropriate cost function for data impact studies. For example, if there were no observations assimilated 48 hours ago, then the trajectory of the 48 and 72 hour forecasts will be the same and their differences will be zero at the verifying analysis time. Observations, however, are usually assimilated and the two forecast trajectories will differ as a result. Forecast error gradients in model space are projected into observation space using the adjoint of the 3DVAR. This yields an observation sensitivity vector $\partial J / \partial \mathbf{y}$, with its elements at the observation locations. $\partial J / \partial \mathbf{y}$ is then used in the observation impact equation:

$\delta \mathbf{e}_{48} = \langle (\mathbf{y} - \mathbf{H}\mathbf{x}_t), \partial J / \partial \mathbf{y} \rangle$, where the brackets represent a scalar inner product and $(\mathbf{y} - \mathbf{H}\mathbf{x}_t)$ is the innovation vector (Langland and Baker, 2004). A negative $\delta \mathbf{e}_{48}$ value indicates a beneficial observation in that assimilation of the observation reduced HyCOM 48 hour forecast error, while a positive $\delta \mathbf{e}_{48}$ value indicates a non-beneficial observation (forecast error actually increased from assimilation of the observation). Non-beneficial impacts are not expected since the assimilation is expected to decrease forecast error by producing improved initial conditions. However, if non-beneficial impacts occur, and they are persistent, then that may indicate problems with the observing system or model performance. Thus, the data impact system can be used as an effective monitoring tool for diagnosing data quality issues or identifying areas where the model has significant predictability limits.

Results

Forecast error gradients are computed daily for differences between 48-hour and 72-hour HyCOM forecasts of temperature, salinity, and the verifying analysis. The 3DVAR adjoint is then executed to obtain the observation sensitivities for use in the observation impact equation. Data impacts are available every day for each observation assimilated and can be partitioned into contributions made by instrument type, geographic domain, and vertical level. Figure 1a shows instantaneous temperature forecast error gradients at the surface. Positive and negative areas of forecast errors are seen indicating that on any given day HyCOM forecast errors are both increasing (positive values) and decreasing (negative values). These patterns will vary with depth and evolve over time in accordance with changes in the observing systems assimilated and the variable skill of the HyCOM forecast. Temperature forecast error gradients averaged over 10 days are shown in Fig. 1b. In general,

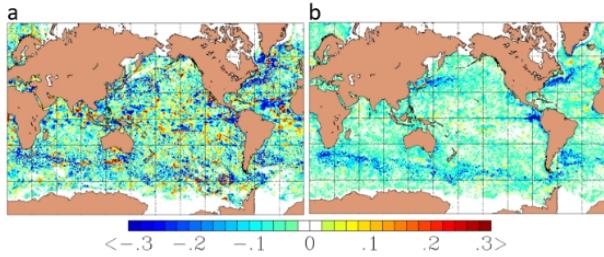


Figure 1. Surface temperature forecast error gradients.

negative values are found almost everywhere, an indication that the assimilation is consistently reducing HyCOM 48-hour forecast error. Beneficial impacts are the greatest in western boundary currents, Antarctic circumpolar current, and eastern tropical Pacific. However, persistent non-beneficial (positive) impact areas are also seen. These areas of forecast error growth could be due to localized, reduced HyCOM predictability arising from instabilities in the system and need further investigation.

It has been demonstrated that routine assimilation of large numbers of observations work together to consistently reduce global HyCOM 48-hour forecast error. An advantage of the adjoint method is that it allows quantification of impacts from the assimilation of individual observations. To summarize these results, impacts

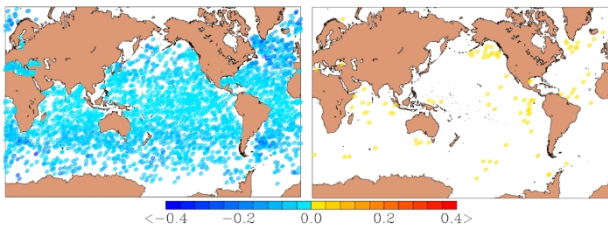


Figure 2. Beneficial (left) and non-beneficial (right) impacts of Argo temperature profiles: 27 Mar – 5 Apr 2021.

are partitioned by data type and averaged over a 10-day period. Impact results presented for any group partition is the sum of all individual observation impacts in that group normalized by the number of observations. Figure 2 shows the locations of beneficial and non-beneficial impacts of Argo temperature profiles assimilated during the 10-day period. A large number of Argo profiles have beneficial impacts from the assimilation, but some Argo profiles have non-beneficial impacts that occur in a fairly random pattern. Figure 3 shows a comparison of the impacts of temperature observations from various

observing systems. Profiles from animal borne sensors are found to have the greatest impact at reducing HyCOM forecast temperature errors, followed by Argo. The animal sensor data are profiles from CTD instruments attached to animals, in particular Elephant Seals. The foraging behavior of the animals brings them to ocean frontal zones in search of food, primarily in hard to reach polar-regions. The seals basically serve as

targeted observing platforms providing high impact data in dynamically sensitive areas.

Summary

The adjoint method has successively been applied to RTOFS-v2 to assess data impacts. The method is computationally efficient and can be used for routine observation monitoring in operations. There is no need to selectively remove observing systems to determine impacts as in a data denial experiment. As such, the method automatically adjusts to changes in the observation suite assimilated as new observing systems are introduced and to changes in the forecast model as model resolution increases or new physics are introduced. It is now possible to efficiently and routinely evaluate the entire global set of oceanographic observations assimilated in RTOFS-v2, determining which data

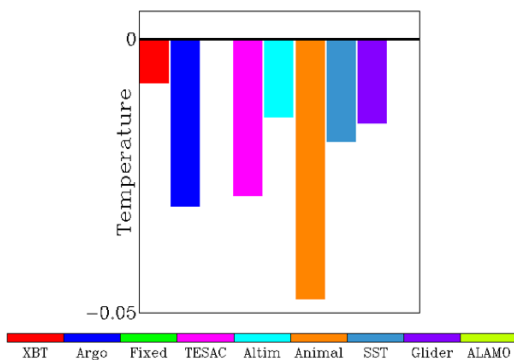


Figure 3. Temperature observing system impacts.

are most valuable and which data are redundant or do not add significant value.

References

Langland, R. and N. Baker, 2004: Estimation of observation impact using the NRL atmospheric variational data assimilation adjoint system. *Tellus* 56A, 189-201.

NOAA-NCEP Next Generation Global Ocean Data Assimilation System (NG-GODAS)

Jong Kim¹, Yi-Cheng Teng¹, Guillaume Vernieres³, Travis Sluka³, Shastri Paturi¹, Yan Hao², Denise Worthen¹, Bin Li², Jun Wang², JieShun Zhu⁴, Hae-Cheol Kim⁵, Daryl Kleist²

¹MSG @ NOAA-NCEP-EMC, ²NOAA-NCEP-EMC, ³JCSDA, ⁴UMD-ESSIC, ⁵UCAR @ GFDL
e-mail: jong.kim@noaa.gov

Efforts to modernize the forecasting systems at the National Oceanic and Atmospheric Administration (NOAA) have resulted in the collaborative development of the Unified Forecasting System (UFS). Comprising the core of future operational systems for global weather, sub-seasonal and seasonal forecasting, the NOAA UFS research to operations (R2O) program builds on several key features, unification of the data assimilation with the Joint Effort for Data Assimilation Integration (JEDI), development of the fully coupled atmosphere-ocean-ice-wave model, modernization of observations processing, modularization and unification of the workflow, and verification of the analysis and forecast. Under the UFS R2O program, the JEDI-based sea-ice ocean coupled assimilation system (SOCA) has been integrated with the Modular Ocean Model version 6 (MOM6, [1]) and the Community Ice Code version 6 (CICE6, [2]) to establish the NG-GODAS system.

We introduce here the NG-GODAS 40 year reanalysis project: experiment configuration, observation data archiving, and preliminary results. In the JEDI object oriented prediction system (OOPS) software structure, the SOCA interface provides a core framework of algorithms that combine generic building blocks for the MOM6 and CICE6 data assimilation application algorithms. A few articles (Trémolet, 2020, Holdaway *et al.*, 2020, and Honeyager *et al.*, 2020) introduce a key concept of the JEDI software system, to highlight how different data assimilation systems can be seamlessly established through the OOPS software infrastructure. A triple horizontal mesh grid, 1° global configuration of the MOM6 model with 75 vertical layers is coupled with the CICE version 6 featuring multiple ice thickness categories and the elastic–viscous–plastic sea ice dynamics model. The initial conditions are set with the OMIP-2 MOM6-SIS2 simulations (Tsujino *et al.*, 2020). The MOM6-CICE6 coupled system is forced with a set of atmospheric fluxes from the NOAA climate forecast system reanalysis (CFSR, 1979–2000) and the global ensemble forecast system (GEFS, 2000-2019).

In addressing the bias issues of the CFSR fluxes, the climatology of the DRAKKAR DFS52 forcing set (Dussin *et al.*, 2014) was applied to adjust precipitation rate, downward shortwave, downward longwave, and wind of the CFSR forcing set. Along with the SOCA MOM6-CICE6 model interfaces, the generic marine observation operators and data handling capabilities of the JEDI unified observation operator and interface for observation data access (IODA) systems are also utilized. In order to unify the various types of file formats and levels of observation data sets, we established a 40 year marine observation database system in the JEDI IODA format.

Table 1 shows satellite and in-situ observation data sets used in the 40 year NG-GODAS reanalysis experiment: satellite sea surface temperature, sea surface salinity, in-situ temperature and salinity, absolute dynamic topography, sea ice concentration, and sea ice freeboard thickness. For the 40 year NG-GODAS reanalysis production run, we have validated the analysis results by comparing them with the current operational ocean monitoring data assimilation systems, GODAS and CFSR. Results are compared against the UK MET office Hadley center EN4.0.2 objective analysis [3] for the time period 2015–2016. In Figure 1, the temperature and salinity mean analysis fields are compared to understand how closely each operational system matches the UK MET office EN4 analysis. Compared against the current operational systems, the NG-GODAS provides considerably improved analysis results. In particular, salinity fields of the NG-GODAS analysis are significantly closer to the EN4 analysis output. This preliminary result demonstrates that the SOCA-based NG-GODAS analysis system is well suited to serve as a building block for the future marine data assimilation system of the NOAA UFS R2O project.

Input stream	Provider	Period	1979	1988	1990	1992	1994	1996	1998	2000	2002	2004	2006	2008	2010	2012	2014	2016	2018	2020
ADT	NESDIS	1993~																		
In-situ T/S	FNMOC	1998~																		
In-situ T/S	WOD	1979~																		
avhrr/sst l3u	NESDIS	2002~2018																		
avhrr/sst l3c	ESA/CCI	1981~2016																		
viirs/sst l3u	NESDIS	2012~																		
windsat/sst l3u	GHRSSST	2004~2018																		
sss/smcp	NASA	2015~																		
sss/smos	NESDIS	2010~																		
sss/aquarius	JPL	2011~2015																		
emc_ice	NCEP	2000~																		
nsidc_ice	NCEP	1988~2015																		
cryosat2_ice	ESA	2010~																		

Table 1. Marine observation data sets assimilated in the NG-GODAS 40 year reanalysis experiment.

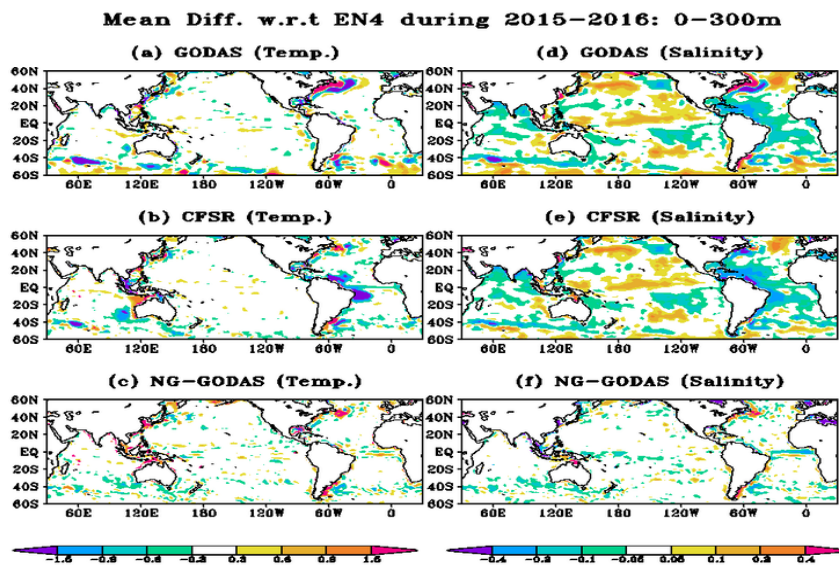


Figure 1. Upper 300m temperature (left columns) and salinity (right columns) mean difference fields for GODAS (top), CFSR (middle) and NG-GODAS (bottom). Differences were computed against EN4.2.

References

- Dussin, R., Barnier, B., Brodeau, L., and Molines, J. M. (2014). The Making of Drakkar Forcing Set DFS5, DRAKKAR/MyOcean Report 01-04-16.
- Holdaway, D., Vernières G., Wlasak M., and King S., 2020: Status of Model Interfacing in the Joint Effort for Data assimilation Integration (JEDI). JCSDA Quarterly, 66, Winter 2020.
- Honeyager, R., Herbener, S., Zhang, X., Shlyayeva, A., and Trémolet, Y., 2020: Observations in the Joint Effort for Data assimilation Integration (JEDI) - UFO and IODA. JCSDA Quarterly, 66, Winter 2020.
- Trémolet, Y., 2020: Joint Effort for Data assimilation Integration (JEDI) Design and Structure. JCSDA Quarterly, 66, Winter 2020.
- Tsujino, H, S Urakawa, Stephen M Griffies, Gokhan Danabasoglu, Alistair Adcroft, A E Amaral, T Arsouze, M Bentsen, R Bernardello, C Böning, A Bozec, E P Chassignet, S Danilov, and Raphael Dussin, et al., August 2020: Evaluation of global ocean–sea-ice model simulations based on the experimental protocols of the Ocean Model Intercomparison Project phase 2 (OMIP-2). Geoscientific Model Development, 13(8), DOI:10.5194/gmd-13-3643-2020.

[1] <https://www.gfdl.noaa.gov/mom-ocean-model>

[2] <https://github.com/CICE-Consortium/CICE>

[3] <https://www.metoffice.gov.uk/hadobs/en4>

Implementation of Ocean Biogeochemical Modeling and Ocean Color Data Assimilation within NOAA/NCEP's Next-Generation Global Ocean Data Assimilation System (NG-GODAS)

Xiao Liu¹ (Xiao.Liu@noaa.gov), Jong Kim¹, Avichal Mehra², Daryl Kleist², Guillaume Vernieres³, Hae-Cheol Kim⁴, Eric Bayler⁵
¹IMSG@ NOAA/NWS/NCEP/EMC, ²NOAA/NWS/NCEP/EMC, ³JCSDA, ⁴UCAR@ NOAA/OAR/GFDL, ⁵NOAA/NESDIS/STAR

Ocean biogeochemical and ecological forecasts provide early warning of ecosystem changes and their impacts on water quality, human health, and/or regional economies, allowing for sufficient lead time to develop mitigation strategies and take corrective actions. Ocean biogeochemical and ecological processes also provide important geophysical feedback to weather and climate systems, through complex ocean biophysical and ocean-atmosphere interactions. The inability to represent ocean biogeochemical and ecological processes and their feedback to oceanic and atmospheric physics in the current generation of operational forecast systems, as well as our limited understanding of the underlying mechanisms of past extreme weather and ecological events, reduces our capability to predict critical weather conditions and ecological “tipping points” and affects management effectiveness at both global and regional scales. Through a project funded by the JPSS Proving Ground and Risk Reduction (PGRR) program, we developed and evaluated ocean biogeochemical modeling and data assimilation tools as well as the required infrastructure at EMC, in support of NOAA/NCEP's operational weather, subseasonal-to-seasonal (S2S), and ecological predictions. This document provides an overview of key milestones of the implementation of an ocean biogeochemical model and the assimilation of satellite-based ocean color observations within NOAA/NCEP's Next-generation Global Ocean Data Assimilation System (NG-GODAS).

1. Ocean biogeochemical modeling

The biogeochemistry model implemented in NG-GODAS is adapted from NOAA/GFDL's BLING model (Biogeochemistry with Light, Iron, Nutrients and Gas version 2, or BLINGv2; Dunne *et al.*, 2020), and is coupled to the Modular Ocean Model version 6 (MOM6; Adcroft *et al.*, 2019) currently being implemented in the Unified Forecast System (UFS). BLINGv2 states are treated essentially as generic tracers in MOM6, and so are subject to advective and diffusive transports, as well as source and sink terms from boundary fluxes (e.g., atmospheric deposition, riverine inputs) and biogeochemical processes (e.g., burial, denitrification). The coupled MOM6-BLINGv2 model has been successfully tested at horizontal resolutions of 1° and 0.25° using NG-GODAS. Preliminary results suggest that upper-ocean physics (e.g., SST) are moderately sensitive to ocean biogeochemical (e.g., Chl-a) variability with a response of up to 1°C in some regions (Figure 1).

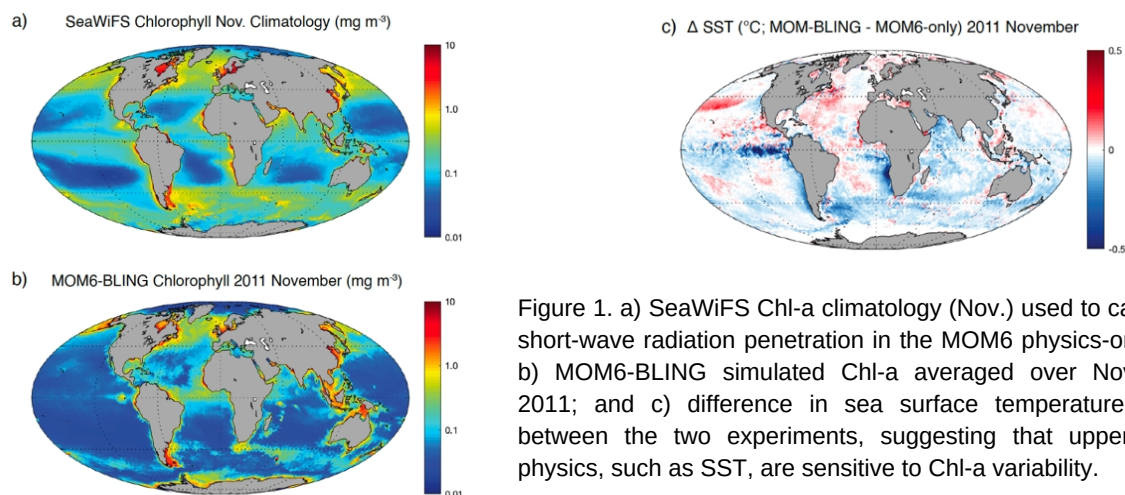


Figure 1. a) SeaWiFS Chl-a climatology (Nov.) used to calculate short-wave radiation penetration in the MOM6 physics-only run; b) MOM6-BLING simulated Chl-a averaged over November 2011; and c) difference in sea surface temperature (SST) between the two experiments, suggesting that upper-ocean physics, such as SST, are sensitive to Chl-a variability.

2. Ocean color data assimilation

NG-GODAS employs the sea-ice ocean and coupled assimilation (SOCA), based on the Joint Effort for Data Assimilation Integration (JEDI). The JEDI project is the backbone for performing data assimilation across the variety of UFS applications. We further developed SOCA to allow the integration of near real-time satellite ocean color products into MOM6-BLINGv2 simulations.

2.1 Ocean color observations

Level-2 data streams have been established from NESDIS into NCEP for NOAA-20/VIIRS and S-NPP/VIIRS historical and near real-time ocean color observations (i.e., chlorophyll concentration, or Chl-a, and particulate organic carbon, or POC), specifically from NOAA CoastWatch and NASA OB.DAAC to NOAA's Research and Development High-Performance Computing System (RDHPCS). The required software to preprocess VIIRS Level-2 ocean color products for basic quality control and ingestion by the JEDI system were developed. Specifically, these observations are converted into a unified data format (i.e., IODA compatible) that can be ingested by any model employing the JEDI system for data assimilation.

2.2. Chl-a and POC analysis

To assimilate Chl-a and POC, the corresponding biogeochemical states saved in the model restart file are updated during each data assimilation cycle (i.e., 24 hrs) based on increments calculated in JEDI/SOCA. Other key states, such as phosphate concentration, are updated by solving BLING internal equations for phytoplankton growth and nutrient limitation based on chl-a or POC increments. The background error covariance ("B") matrix for the ocean color observations will be computed using the "Background error on Unstructured Meshgrid" (BUMP) in the SABER package of JEDI, and is assumed to be diagonal. For each grid-point, the observational error variance will be set to be proportional to the observed values (e.g., observational error = 30% for Chl-a; Tsiaras *et al.*, 2017). The UFOs will estimate "ocean color" properties from the biogeochemical model as the corresponding variables averaged over the first optical depth at each grid-point. Figure 2 shows a preliminary Chl-a daily analysis using the 3-dimensional variational (3DVAR) scheme.

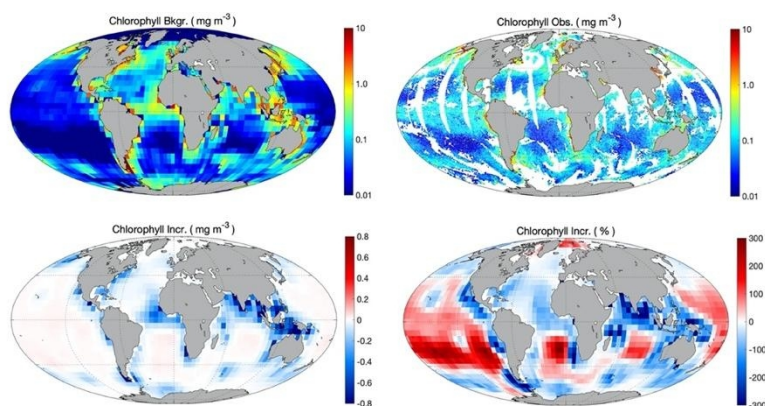


Figure 2. (upper panels) Simulated "background" Chl-a in MOM6-BLING and Level-2 Chl-a derived from NOAA-20/VIIRS imagery on 2018/04/15, used for Chl-a assimilation; (lower panels) Chl-a increments calculated based on the 3DVAR scheme in

References

- Adcroft, A., Anderson, W., Balaji, et al. (2019). The GFDL global ocean and sea ice model OM4.0: Model description and simulation features. *Journal of Advances in Modeling Earth Systems*, 11, 3167– 3211.
- Dunne, John P., I Bociu, Benjamin Bronselaer, et al. (2020). Simple Global Ocean Biogeochemistry with Light, Iron, Nutrients and Gas version 2 (BLINGv2): Model description and simulation characteristics in GFDL's CM4.0. *Journal of Advances in Modeling Earth Systems*. DOI:10.1029/2019MS002008.
- Tsiaras, K. P., Hoteit, I., Kalaroni, S., Petihakis, et al. (2017). A hybrid ensemble-OI Kalman filter for efficient data assimilation into a 3-D biogeochemical model of the Mediterranean. *Ocean Dynamics*, 67(6), 673– 690.

Data Used in Global Ocean Modeling and Data Assimilation Systems at NOAA/NCEP

Shastri Paturi, Yan Hao, Jong Kim
IMSG @ NOAA/NWS/NCEP/EMC, College Park, MD 20740
Email: Shastri.Paturi@noaa.gov

The National Centers for Environmental Prediction (NCEP) develops and delivers operational environmental forecasting systems to its partners within NOAA (e.g., NOS, NHC, etc.) and externally (e.g., US Coast Guard). These operational systems are driven by large earth observing systems that measure various parameters. Observation data sets are received by NCEP Central Operations (NCO) through the Global Telecommunication System (GTS) in BUFR format and from the NOAA/NESDIS operational server (PDA - Production Distribution and Access) in netCDF format and are saved on the dcom server and in individual data tanks based on the source of the measurement (e.g., BATHY, TESAC, SUBPFL, SHIPS, etc.). BUFR decoders are used to read the data from the BUFR file using the pneumonics of certain types of data header file [1].

The marine data observations in BUFR format consist of in-situ temperature and salinity and sea-ice concentration and observations in netCDF format consist of satellite sea surface temperature (SST), sea surface salinity (SSS) and absolute dynamic topography (ADT). These data are then converted into model specific formats to be ingested by each model's data assimilation system. This involves model specific data conversion efforts and data storage problems. Requirements for observation files and I/O handling involved in different modeling and data assimilation workflows are incredibly diverse. Creating a common software system for organizing and storing the vast amounts of observation data is highly desirable to maintain current and future operational forecast systems in a sustainable way.

As part of a modernisation effort of the ocean forecasting systems under the umbrella of the NOAA unified forecast system (UFS) program, a data unification project has been started with the Joint Effort for Data Assimilation Integration (JEDI) to establish a model agnostic method of sharing observation data and exchanging modeling and data assimilation results. The Interface for Observation Data Access (IODA) is a subsystem of JEDI that handles data processing and provides for a common data format in netCDF. This allows for the long-term storage of data and the creation of historical databases. The underlying structure of the IODA format is to represent the variables (e.g., temperature, salinity, etc.) in columns and the locations in rows. Metadata tables are associated with each axis of the data tables and the location metadata hold the values describing each location, and which are appropriate for each observation type (e.g., latitude, longitude). Actual data values are contained in the third dimension of the IODA data table: observation values, observation error, quality control flags, and simulated observation values of $H(x)$ at different stages of the data assimilation process. The python-based IODA converters for all the marine surface and profile observation data types described above have been successfully developed and merged into the JEDI repository.

A 40-year historical IODA-based database of the marine observations were collected for the 1° global reanalysis experiment of the NOAA-NCEP Next Generation Global Ocean Data Assimilation System (NG-GODAS), described in Jong-Kim et al., (2021). The database covers the period 1979-2020. Table 1 describes each parameter, source, datatype and period of data availability. The goal of this project is to create an expandable database of quality controlled observations for 40 years to be used for development, experimentation and reanalysis. These archived observational datasets will be used to develop the necessary observation quality control schemes through the JEDI Unified Forward Operator (UFO), which does the comparison between the observations and the forecast model through $H(x)$ calculation (Honeyager et al., 2020). Figure 1 shows an example of the JEDI-based UFO application result from the AVHRR SST data sets in the NG-GODAS reanalysis experiment.

Datatype	Satellite/sensor	Source	Availability	Data Level
Sea Surface Temperature	NOAA/AVHRR	ESA-CCI http://anon-ftp.ceda.ac.uk/inmcm2/esa/cci/sst/data/CDR_v2/AVHRR/3U/v2/	1981-2015	L3U
	NOAA/AVHRR	pathfinder http://ftp.nodc.noaa.gov/pub/data/nodc/pathfinder/Version5.3/3C/	1981-2020	L3C
	NOAA/AVHRR	NOAA/NESDIS http://ftp.star.nesdis.noaa.gov/pub/socd2/coastwatch/sst/avhrr_gac/	2002-2018	L3U
	METOPA/AVHRR	https://podanc-tools.jpl.nasa.gov/drive/files/allData/ghrsst/data/GDS2/L3U/AMSR2/	2004-2020	L3U
	GCOM-W/AMSR2	https://podanc-tools.jpl.nasa.gov/drive/files/allData/ghrsst/data/GDS2/L3U/WindSat/	2004-2020	L3U
	Coriolis/WindSat	https://podanc-tools.jpl.nasa.gov/drive/files/allData/ghrsst/data/GDS2/L3U/GMI/	2014-2020	L3U
In-situ Temperature & Salinity	ARGO; buoys (drifting & moored); CTD; MBT; XBT; ship	WOD https://data.nodc.noaa.gov/wna/WOD/YEARLY/	1979-2020	
Sea Surface Salinity	SMAP	NASA/JPL https://podanc-opendap.jpl.nasa.gov/opendap/hyrax/allData/smap/L2/PL/V4.3/	2015-2020	L2
	SMOS	ESA https://smaos.esa-diss.eo.esa.int/	2010-2020	L2
ICE Concentration	DMSP/n07; f08; f11; f13; f17	NSIDC https://www.ncei.noaa.gov/data/sea-ice-concentration/access/	1979-2015	L3
	DMSP/SSMR; SSM/I; SSMIS (285, 286 GHZ)	L1b BUFR converted to L2 nc files*	2003-2020	L2
ICE freeboard	cryosat	ftp://science-pds.cryosat.esa.int/SIR_GDR/	2010-2020	
Absolute dynamic Topography	Jason-1,2; AltiKa; Sentinel 3A,3B;	NOAA/NESDIS	1993-2020	
	TOPEX/POSEIDON; Envisat	http://ftp.star.nesdis.noaa.gov/pub/sod/isa/trds/adt/		

SMAP: Soil Moisture Active Passive
SMOS: Soil Moisture Ocean Salinity
* NOAA-NEP-EMC C++ converter provided by Robert Grumbine
DMSP: Defense Meteorological Satellite Program
JPL: Jet Propulsion Laboratory
NSIDC: National Snow and Ice Data Center
WOD: World Ocean Database
ESA/CCI: European Space Agency/Climate Change Initiative

Table 1: 40 year marine observation datasets archived in JEDI-IODA format.

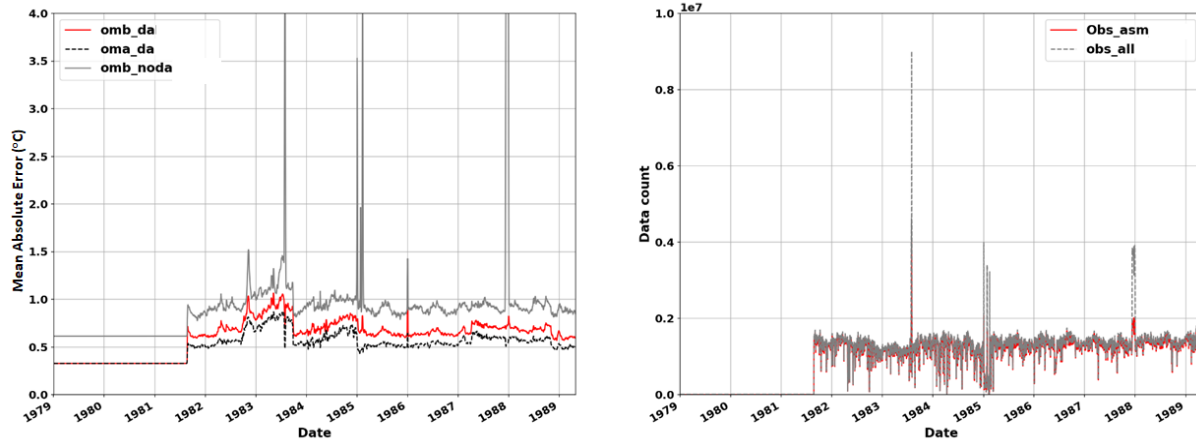


Figure 1. Left panel is time series statistics of the satellite SST observation-analysis (oma) and observation-background (omb). Right panel is data counts for assimilation and no assimilation. 1deg experiment. AVHRR ESA-CCI data sets are applied for the time period 1979~1990.

References

Honeyager, R., Herbener, S., Zhang, X., Shlyayeva, A., and Trémolet, Y., 2020: Observations in the Joint Effort for Data assimilation Integration (JEDI) - UFO and IODA. JCSDA Quarterly, 66, Winter 2020.

Jong Kim, Yi-Cheng Teng, Guillaume Vernieres, Travis Sluka, Shastri Paturi, Yan Hao, Denise Worthen, Bin Li, Jun Wang, JieShun Zhu, Hae-Cheol Kim, Daryl Kleist, NOAA-NCEP Next Generation Global Ocean Data Assimilation System (NG-GODAS), Blue Book, 2021.

[1] <https://emc.ncep.noaa.gov/emc/pages/infrastructure/bufrlib.php>

Variability of water and heat exchanges through the Bering Strait in numerical experiments with the NEMO/SI3 model assimilating observational data

B.S. Strukov, Yu.D. Resnyanskii, A.A. Zelenko, V.N. Stepanov

Hydrometeorological Research Centre of Russian Federation

Email: bsstr@mail.ru

Introduction

The most detailed representation about the variability of the dynamic structure of the ocean can be derived from the results of calculations using hydrodynamic models with the assimilation of available observational data. NEMO model (NEMO ocean engine) coupled with the thermodynamic sea ice model (The NEMO Sea Ice Working Group, 2018) is one of the most advanced and widely used ocean models. In the latest versions, starting from 4.0, it is possible to embed the AGRIF library (Blayo and Debreu, 1999), including also a sea ice model with several ice categories. The software of the library allows performing calculations simultaneously within a single task on several grids: a global, relatively coarsely resolved grid (hereafter “*host*”), is combined with a regionally confined, high-resolution grid (hereafter “*nest*”) allowing for two-way interactions: the *host* not only provides boundary conditions for the *nest* but also receives information from the *nest*.

Within the framework of this approach, calculations were carried out to reproduce the circulation of the subpolar part of the Pacific Ocean. In particular, the model results allow tracing the characteristics of seasonal and interannual variability of water and heat exchange through the Bering Strait.

Model configuration and data used

The combined grid area of the model consists of a *host* at $1 \times 1^\circ$ horizontal resolution within ORCA1 (362 \times 332 nodes) and 75 vertical levels and an embedded *nest* at about 0.25° resolution, covering the subarctic part of the Pacific Ocean, the Bering Sea, the Alaska Bay, and also part of the Arctic basin up to latitude 80°N . The multi-category ice model SI3 included five thickness categories: <0.6 m; 0.6 - 1.3 m; 1.3 - 2.2 m; 2.2 - 3.8 m and > 3.8 m.

A numerical experiment with a two-grid configuration of the model domain forced by DFS5.2 (DRAKKAR Forcing Sets) included two stages: 1) the 6-year long spin-up integrations from 1995 to 2000, initialized with January temperature and salinity from the WOA13 Atlas and an ocean at rest, and 2) the ocean states at the end of the spin-up integrations are used to initialize the simulation for the period 01.01.2001–29.12.2015 assimilating data of vertical distributions of temperature and salinity of water by Argo buoys (<ftp://ftp.ifremer.fr/ifremer/argo/geo>), satellite measurements of SST (<ftp://ftp.nodc.noaa.gov/pub/data.nodc/pathfinder/Version5.2/>) and data of sea ice extent (<ftp://ftp.ifremer.fr/ifremer/cersat/products/gridded/psi-concentration/data>).

Data assimilation was carried out using a sequential cyclic scheme (Zelenko et al., 2016) and three-dimensional variational analysis (Tsyrlunikov et al., 2010) with a 10-day assimilation window.

Water and heat exchange through the Bering Strait

Water and heat exchange through the Bering Strait (that in the model domain is located in the *nest* with the horizontal resolution of 0.25°) is one of the key elements of global circulation, since the dynamics of the eastern Arctic and the adjacent North Pacific waters significantly depends on the rate of transports of mass, heat and salt through this strait.

The calculations show that the mass transport through the strait section is about 0.76 Sv ($1 \text{ Sv} = 10^6 \text{ m}^3/\text{s}$) with a sufficiently large temporal variability reaching the maximum transport value up to 5.5 Sv (the root-mean-square deviation (RMS) is 0.90 Sv). There is a negative time trend of ~ -0.0227 Sv per year, indicating a slowdown in the rate of water inflow from the Pacific Ocean into the Arctic basin (Fig. 1a). The mean transport through the strait is in good agreement with the available measurements (0.8 Sv) (Roach et al., 1995; Woodgate et al., 2005) and with model values in similar works, e.g. see (Kinney et al., 2014).

Heat transport is characterized by a clearly pronounced seasonal variability that is superimposed by short-term variations (Fig. 1b). Its RMS of 1.90×10^{13} W exceeds the average value of the heat transport for the whole period of 1.25×10^{13} W against the backdrop of a slight negative trend of -2.22×10^{11} W per year.

Seasonal changes of the volume transport averaged for the period 2001–2015 are weak and the transport is most often directed from the Pacific Ocean to the Arctic basin with episodic changes in the direction of the flow (Fig. 2a). Such changes of directions most often occur in the autumn-winter period (from October to January). The heat transport is most intense in the summer-autumn period from July to October, and its greatest interannual variability is in the period from May to December (Fig. 2b).

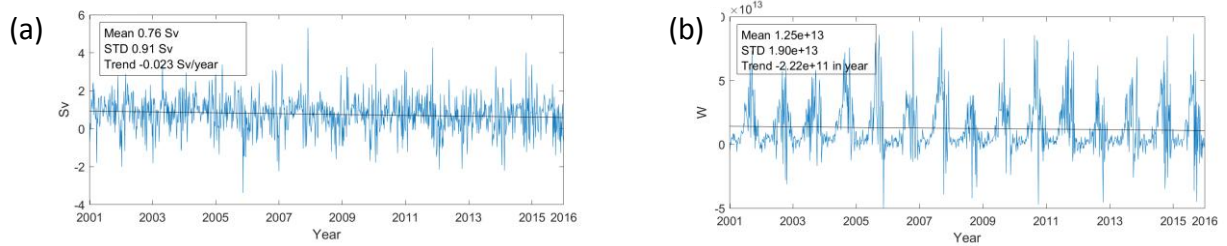


Fig. 1. The variability of volume transport (in Sv, $1 \text{ Sv} = 10^6 \text{ m}^3/\text{s}$) (a) and heat flux (in 10^{13} W) referred to reference temperature of -2.6°C (b) through the Bering Strait section according to the numerical experiment for 2001–2015. Positive values correspond to a transport from south to north.

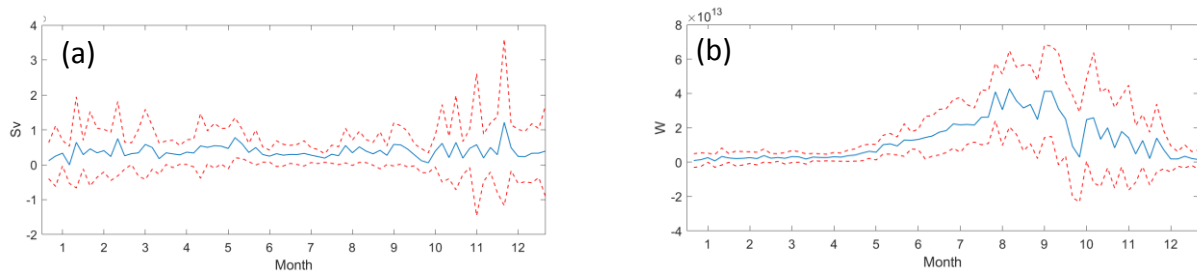


Fig. 2. Seasonal changes in water (a) and heat (b) exchanges through the Bering Strait averaged for 2001–2015 (blue lines). The red dashed lines show the standard deviations in water and heat transports.

Summary

The presented version of modelling the subarctic zone of the Pacific Ocean and the southeastern part of the Arctic with NEMO ocean model coupled with the SI3 sea ice model using the AGRIF library for nested grids together with data assimilation allows tracing the dynamics of water and heat exchange through the Bering Strait, which is one of the key regions of the interoceanic water exchange.

The model results are quite satisfactory when compared to observations and it shows the realism of the resulting model output of the data assimilation system with the detailing of individual water basin and, therefore, it indicates that such approach is promising for obtaining a detailed picture of the ocean states with moderate computational costs.

References

- Blayo E. and Debreu L., 1999: Adaptive mesh refinement for finite-difference ocean models: First experiments. *J. Phys. Oceanogr.* **29**(6). 1239–1250.
- NEMO ocean engine, Scientific Notes of Climate Modelling Center, 27 — ISSN 1288-1619, Institut Pierre-Simon Laplace (IPSL), doi:10.5281/zenodo.1464816/
- The NEMO Sea Ice Working Group, 2018: SI3 – Sea Ice modelling Integrated Initiative – The NEMO Sea Ice Engine, Note du P'ole de mod'elisation, Institut Pierre-Simon Laplace (IPSL), France, No XX, ISSN No 1288-1619.
- Roach A. T., Aagaard K., Pease C. H., Salo S. A., Weingartner T., Pavlov V., and Kulakov M., 1995: Direct measurements of transport and water properties through Bering Strait. *J. Geophys. Res.* **100**. 18,443–18,457.
- Tsyrlunikov M.D., Svirenko P.I., Gorin V.E., Gorbunov M.E., and Klimova E.G., 2010: Development of three-dimensional variational data assimilation scheme in the Hydrometeorological Center of Russia. In: 80 Let Gidrometsentru Rossii, Moscow: Triada LTD. 21–35. (in Russian)
- Woodgate R.A., Aagaard K. and Weingartner T.J., 2005: Monthly temperature, salinity, and transport variability of the Bering Strait throughflow. *Geophys Res Lett* 32:L04601. doi:10.1029/2004GL021880.
- Kinney Clement, Maslowski J., Aksenov W., de Cuevas Y., Jakacki B., Nguyen J., Osinski A., Steele R., Woodgate M., and Zhang R.A., 2014: On the flow through Bering Strait: a synthesis of model results and observations. In: Grebmeier, J. (ed.) *The Pacific-Arctic Region: ecosystem status and trends in a rapidly changing environment*. Dordrecht, NL. Springer. 167–198.
- Zelenko A.A., Vil'fand R.M., Resnyanskii Y.D., Strukov B.S., Tsyrlunikov M.D. and Svirenko P.I., 2016: An ocean data assimilation system and reanalysis of the world ocean hydrophysical fields. *Izvestiya. Atmospheric and Oceanic Physics.* **52**(4). 443–454. DOI: 10.1134/S0001433816040149.

Implementation of Forcing-Bias Correction for the JEDI-Based Next Generation Global Ocean Data Assimilation System (NG-GODAS)

Yi-Cheng Teng¹, Jong Kim¹, Travis Sluka³ and Daryl Kleist²

¹IMSG at NOAA/NWS/NCEP/EMC, College Park, Maryland, USA; ²NOAA/NWS/NCEP/EMC, College Park, Maryland, USA; ³JCSDA, Boulder, Colorado, USA

Email: yi-cheng.teng@noaa.gov

Introduction

The National Weather Service (NWS) is building a coupled modeling system that will form the core of its operational models for global weather (GFS), sub-seasonal (GEFS) and seasonal (SFS) forecasting. The new coupled model under development is a part of NOAA's Unified Forecast System (UFS), consisting of the FV3 dynamical core for the atmosphere, MOM6 for the ocean, CICE6 for the sea-ice, and WW3 for waves. In the current setup, ocean initial conditions are obtained from the existing operational Global Ocean Data Assimilation System (GODAS) [1], which uses an older generation ocean model (MOM3 at 1-deg resolution) and the 3DVar ocean DA implemented in 2003. As part of ongoing efforts to improve forecasting, the NCEP's Environmental Modeling Center (EMC) is developing a prototype version of the JEDI-based Next Generation Global Ocean Data Assimilation System (NG-GODAS). The NG-GODAS uses SOCA (Sea-ice Ocean Coupled Assimilation) as its ocean data assimilation component, and a more advanced ocean model (MOM6 at 1/0.25-deg resolution). The NG-GODAS is forced with a set of atmospheric fluxes from CFSR [2]. However, there exist very large known biases in the CFSR fluxes. For example, in the western tropical Pacific and Indian oceans, the downward shortwave radiation from CFSR is too high compared to other reanalysis products that have been calibrated to fit observations [3]. The original GODAS used a very strong SST relaxation, which likely mitigated the effect of forcing biases. However, the NG-GODAS will not use any SST relaxation, so these forcing biases must be appropriately addressed.

Methodology

To overcome this CFSR forcing bias issue, a climatological correction approach proposed in Sluka [3] is implemented in NG-GODAS. The monthly climatology of the DRAKKAR forcing set (DFS52) [4] is used to correct the CFSR monthly climatology. First, we calculated the monthly climatologies for both the DFS52 and CFSR. Then, two different types of correction factors are considered. The multiplicative factor is used for fields that should not become negative (e.g., downward long/short wave, precipitation). An additive correction factor is used for the 10m zonal/meridional wind so that in high wind events (e.g., Hurricanes) the wind fields won't receive an overly large increase in intensity as they would with a multiplicative correction factor. One degree NG-GODAS-free-runs (no data assimilation) with and without bias correction from 1988-1999 are conducted and the results are presented in this report to evaluate the performance of the bias correction factors.

Results

By applying the forcing bias-correction factors to the free-run NG-GODAS, modeled SST with lower bias is produced when compared to the OISSTV2 dataset (Figure1). The mean absolute error (MAE) was reduced from 0.52°C to 0.43°C, and the root mean square error (RMSE) was reduced from 0.73°C to 0.59°C. We further checked the northward global ocean heat transport from simulations with and without bias correction. In Figure 2, after applying the climatological correction the CFSR (red line) exhibits similar northward global ocean heat transport compared to the runs using other forcing (CORE-II and GEFS) along the latitudes.

Summary

The preliminary results show that modeled results are improved after applying the forcing bias correction. The forcing bias-correction approach reported here is relatively easy to apply to other forcing datasets. Currently, this bias correction has been implemented in the NG-GODAS 40-year reanalysis experiment.

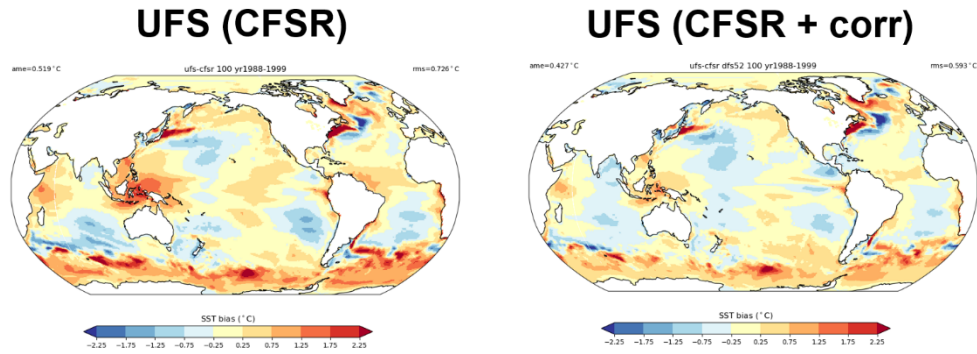


Figure 1: Difference in the ocean SST from free-run NG-GODAS compared with OISST, averaged over 1988-1999. Left: using uncorrected CFSR fluxes (left); Right: CFSR fluxes with bias correction.

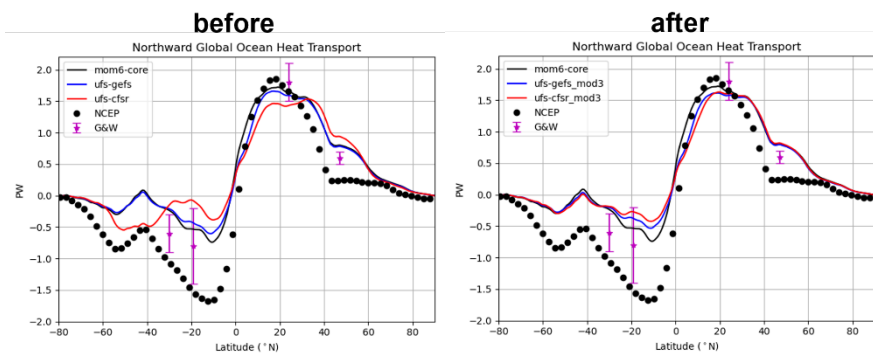


Figure 2: Directly calculated 2000 mean northward global ocean heat transport from CORE-II, GEFS, and CFSR simulations. Also shown are the implied mean northward global ocean heat transport derived from air-sea surface heat fluxes using NCEP reanalysis data (NCEP) and the observation-based in situ estimates (Ganachaud & Wunsch, 2003 [5], G&W). CORE = Coordinated Ocean-sea ice Reference Experiments.

References

- [1] Behringer, D. and Xue, Y. (2004). Evaluation of the Global Ocean Data Assimilation System at NCEP: The Pacific Ocean. In Eighth Symposium on Integrated Observing and Assimilation Systems for Atmosphere, Oceans, and Land Surface, AMS 84th Annual Meeting, number January, pages 11–15.
- [2] Saha, S., Moorthi, S., Wu, X., Wang, J., Nadiga, S., Tripp, P., Behringer, D., Hou, Y.-T., Chuang, H.-y., Iredell, M., Ek, M., Meng, J., Yang, R., Mendez, M. P., van den Dool, H., Zhang, Q., Wang, W., Chen, M., and Becker, E. (2014). The NCEP Climate Forecast System Version 2. *Journal of Climate*, 27(6):2185–2208.
- [3] Sluka, T. C. (2018). Strongly coupled ocean-atmosphere data assimilation with the local ensemble transform Kalman filter. Ph.D. dissertation. College Park: University of Maryland.
- [4] Dussin, R., Barnier, B., Brodeau, L., and Molines, J. M. (2016). The Making Of the DRAKKAR FORCING SET DFS5. DRAKKAR/MyOcean Report 01-04-16, April:1–34.
- [5] Girton, J. B., & Sanford, T. B. (2003). Descent and modification of the overflow plume in the Denmark Strait. *Journal of Physical Oceanography*, 33(7), 1351–1364.